Ru-Zn Heteropolynuclear Complexes Containing a Dinucleating Bridging Ligand: Synthesis, Structure and Isomerism.

Lorenzo Mognon,[a] Jordi Benet-Buchholz,[a] S. M. Wahidur Rahaman,[a] Carles Bo[a,*] and Antoni Llobet[a,b,*]

a Institute of Chemical Research of Catalonia (ICIQ), Avinguda Països Catalans 16, 43007 Tarragona, Spain
b Departament de Química, Universitat Autònoma de Barcelona, Cerdanyola del Vallès, 08193 Barcelona, Spain

Abstract

Mononuclear complexes *in-* an *out*-[Ru(Cl)(trpy)(Hbpp)]$^+$ (***in*-0**, ***out*-0**; Hbpp is 2,2'-(1H-pyrazole-3,5-diyl)dipyridine and trpy is 2,2':6',2"-terpyridine) are used as starting materials for the preparation of Ru-Zn hetero dinuclear *out*-{[Ru(Cl)(trpy)][ZnCl$_2$](µ-bpp)} (***out*-2**) and heterotrinuclear *in,in*- and *out,out*-{[Ru(Cl)(trpy)]$_2$(µ-[Zn(bpp)$_2$])}$^{2+}$ (***in*-3**, ***out*-3**) constitutional isomers. Further the substitution of the Cl ligand from the former complexes leads to Ru-aqua *out,out*-{[Ru(trpy)(H$_2$O)]$_2$(µ-[Zn(bpp)$_2$])}$^{4+}$ (***out*-4**) and the oxo-bridged Ru-O-Ru complex *in,in*-{[Ru^{III}(trpy)]$_2$(µ-[Zn(bpp)$_2$(H$_2$O)]µ-(O)}$^{4+}$ (***in*-5**). All complexes are thoroughly characterized by the usual analytic techniques as well as by spectroscopy by means of UV-vis, MS and when diamagnetic by NMR. CV and DPV are used to extract electrochemical information and monocrystal X-ray diffraction to characterize complex ***out*-2**, ***in*-3**, ***out*-3** and ***in*-5** in the solid state. Complex ***out*-3** photochemically isomerizes towards ***in*-3**, as can be observed by NMR spectroscopy and rationalized by Amsterdam Density Functional calculations.

Keywords: synthesis, coordination complexes, constitutional isomerization, transition metal complexes, light induced isomerization

Introduction

Polynuclear transition metal complexes are a very interesting class of complexes whose properties can be tuned by the type of the bridging ligands bonded to the transition metals. The bridging ligand thus dictates the degree of electronic communication between two or more transition metals. In addition the structure of the ligand can generate a particular spatial disposition of the metal centers that can favor a cooperative effect for a given reaction.[1] Taking into account the relatively large number of transition metals and the huge variety of bridging ligands, an immense number of complexes can be potentially obtained with a large diversity of properties.

Polynuclear transition metal complexes have found interesting application in fields where cooperation between metal centers is important such as: magneto-chemistry,[2] optical properties,[3] reactivity,[1d] catalysis[4,5] etc. Nature also benefits from metal cooperation in a number of metalloproteins whose functions range from small molecule activation (N_2, O_2, and H_2)[6] to hydrolysis.[6d, 7] Low-molecular-weight models have been proven crucial in some cases for the understanding of the spectroscopic and structural properties of the active site of these proteins.[7g, 8]

A fundamental characteristic of coordination complexes is the multiple different type of isomers that they can display. Regarding Ru complexes containing the Hbpp ligand (Hbpp is 2,2'-(1H-pyrazole-3,5-diyl)dipyridine) we have previously described examples where Ru-dmso linkage isomerism takes place induced by a change in oxidation state.[9] We have also described the presence of axial chirality due to the through space supramolecular interaction and different ligand space arrangement in Ru-Hbpp complexes containing the MeCN ligand.[10] In addition we have also described constitutional isomerism in mononuclear Ru-Hbpp complexes containing the tridentate meridional 2,2':6',2''-terpyridine (trpy) ligand and Cl or H_2O ligands in the case of *in*-an *out*-[Ru(Cl)(trpy)(Hbpp)]$^+$ (***in*-0**, ***out*-0**) and *in*- an *out*-[Ru(trpy)(Hbpp)(H_2O)]$^{2+}$ (***in*-1**, ***out*-1**).[11]

The non-symmetric nature of the Hbpp ligand allows to easily prepare mononuclear complexes and use the latter as starting materials for the preparation of the

corresponding multinuclear complexes. On the other hand symmetric ligands generally lead to homodinuclear complexes and sometimes to even coordination oligomers or polymers[12] especially with first row transition metal complexes.

Here on we present the synthesis and reactivity of new hetero di and trinuclear complexes containing the bpp[-] ligand, using the corresponding mononuclear Ru-Hbpp complexes, *in*-0 and *out*-0, as synthetic intermediates.

Experimental section

Preparations. The starting complexes *out*-[Ru(Cl)(Hbpp)(trpy)](PF$_6$), **out-0** and *in*-[Ru(Cl)(Hbpp)(trpy)](PF$_6$), **in-0** and their respective aqua complexes *out*-[Ru(Hbpp)(trpy)(H$_2$O)](ClO$_4$)$_2$, **out-1** and *in*-[Ru(Hbpp)(trpy)(H$_2$O)](ClO$_4$)$_2$, **in-1** were prepared as described in the literature.[11a]

***out*-{[Ru(Cl)(trpy)][ZnCl$_2$](μ-bpp)}·H$_2$O, *out*-2·H$_2$O.** A 100 mg (0.132 mmol) sample of *out*-[Ru(Cl)(Hbpp)(trpy)](PF$_6$) was dissolved in 40 mL of methanol, and then 19.0 mL of triethylamine (0.136 mmol) was slowly added to the solution under magnetic stirring and heating at 50 ºC. Afterwards, 90 mg of ZnCl$_2$ (0.660 mmol) previously dissolved in 10 mL of methanol was added, and the solution was kept stirring for 1 h at 50 ºC. A black solid is then filtered from the solution, and washed with methanol (3 x 10 mL) and ether (3 x 10 mL). Yield: 89 mg (92.8%). Anal. Calcd for C$_{28}$H$_{20}$Cl$_3$N$_7$RuZn·H$_2$O: C, 45.12; H, 2.98; N, 13.15. Found: C, 44.90; H, 2.66; N, 12.96. ^{1}H NMR (400MHz, d_6-DMSO): δ = 9.92 (d, $^3J_{16-17}$ = 5.5 Hz, H16), 8.57 (d, $^3J_{7-8}$ = $^3J_{9-8}$ = 8.3 Hz, H7, H9), 8.48 (d, $^3J_{4-3}$ = $^3J_{12-13}$ = 7.9 Hz, H4,H12), 8.30 (d, $^3J_{19-18}$ = 7.6 Hz, H19), 8.19 (dd, $^3J_{18-19}$ = 7.6 Hz, $^3J_{18-17}$ = 7.4 Hz, H18), 8.11 (d, $^3J_{28-27}$ = 4.5 Hz, H28), 8.03 (dd, $^3J_{26-25}$ = 8.0 Hz, $^3J_{26-27}$ = 7.9 Hz, H26), 7.97 (t, $^3J_{8-7}$ = $^3J_{8-9}$ = 8.3 Hz, H8), 7.85 (dd, $^3J_{3-4}$ = $^3J_{13-12}$ = 7.9 Hz, $^3J_{3-2}$ = $^3J_{13-14}$ = 7.8 Hz, H3, H13), 7.79 (d, $^3J_{25-26}$ = 8.0 Hz, H25), 7.74 (s, H22), 7.72 (dd, $^3J_{17-18}$ = 7.4 Hz, $^3J_{17-16}$ = 5.5 Hz, H17), 7.56 (d, $^3J_{1-2}$ = $^3J_{15-14}$ = 5.2 Hz, H1, H15), 7.37 (dd, $^3J_{27-26}$ = 7.92, $^3J_{27-28}$ = 4.5 Hz, H27), 7.29 (dd, $^3J_{2-3}$ = $^3J_{14-13}$ = 7.8 Hz, $^3J_{2-1}$ = $^3J_{14-15}$ = 5.2 Hz, H2, H14). NMR is assigned following the labels in Figure 1. MALDI-MS (CH$_2$Cl$_2$): m/z = 727.0 ([M]$^+$). Cyclic Voltammetry (CH$_2$Cl$_2$, TBAH): E$_{1/2}$ = 0.543 V *vs.* SSCE (ΔE = 76 mV).

***out,out*-{[Ru(Cl)(trpy)]$_2$(μ-[Zn(bpp)$_2$])}(PF$_6$)$_2$·H$_2$O, *out*-3·H$_2$O.** A 80 mg (0.110 mmol) sample of *out*-{[Ru(Cl)(trpy)][ZnCl$_2$](μ-bpp)} was dissolved in the minimum amount of DMF, then a few drops of a saturated aqueous KPF$_6$ solution were added. Afterwards water was added until a precipitate appeared. The mixture was cooled in fridge for 2 hours, and then the solid filtered on a frit and washed with water (3 x 10 mL) and ether (3 x 10 mL). Yield: 75 mg (88.7%). Anal. Calcd for C$_{56}$H$_{40}$Cl$_2$F$_{12}$N$_{14}$P$_2$Ru$_2$Zn·H$_2$O: C, 43.24; H, 2.72; N, 12.61. Found: C, 43.33; H, 2.69; N, 12.47. ^{1}H NMR (400MHz, d_6-acetone): δ = 9.82 (d, $^3J_{16\text{-}17}$ = $^3J_{41\text{-}40}$ = 5.1 Hz, H16, H41), 8.65 (d, $^3J_{19\text{-}18}$ = $^3J_{38\text{-}39}$ = 7.7 Hz, H19, H38), 8.40 (dd, $^3J_{18\text{-}17}$ =$^3J_{39\text{-}40}$ = 7.7 Hz, $^3J_{18\text{-}19}$ = $^3J_{39\text{-}38}$ = 7.7 Hz, H18, H39), 8.36 (dd, $^3J_{26\text{-}25}$ = $^3J_{31\text{-}32}$ = 7.9 Hz, $^3J_{26\text{-}27}$ = $^3J_{31\text{-}30}$ = 7.9 Hz, H26, H31), 8.23 (d, $^3J_{28\text{-}27}$ = $^3J_{29\text{-}30}$ = 4.9 Hz, H28, H29), 8.16 (d, $^3J_{7\text{-}8}$ = $^3J_{50\text{-}49}$ = 8.0 Hz, H7, H50), 8.15 (d, $^3J_{4\text{-}3}$ = $^3J_{53\text{-}54}$ = 7.8 Hz, H4, H53), 8.11 (d, $^3J_{12\text{-}13}$ = $^3J_{45\text{-}44}$ = 7.9 Hz, H12, H45), 8.10 (d, $^3J_{25\text{-}26}$ = $^3J_{32\text{-}31}$ = 7.9 Hz, H25, H32), 8.07 (s, H22, H35), 7.79 (dd, $^3J_{17\text{-}18}$ = $^3J_{40\text{-}39}$ = 7.7 Hz, $^3J_{17\text{-}16}$ = $^3J_{40\text{-}41}$ = 5.1 Hz, H17, H40), 7.77 (d, $^3J_{9\text{-}8}$ = $^3J_{48\text{-}49}$ = 7.6 Hz, H9, H48), 7.74 (dd, $^3J_{13\text{-}12}$ = $^3J_{44\text{-}45}$ = 7.9 Hz, $^3J_{13\text{-}14}$ = $^3J_{44\text{-}43}$ = 7.8 Hz, H13, H44), 7.64 (dd, $^3J_{27\text{-}26}$ = $^3J_{30\text{-}31}$ = 7.9 Hz, $^3J_{27\text{-}28}$ = $^3J_{30\text{-}29}$ = 4.9 Hz, H27, H30), 7.57 (d, $^3J_{1\text{-}2}$ = $^3J_{56\text{-}55}$ = 5.3 Hz, H1, H56), 7.43 (dd, $^3J_{2\text{-}3}$ = $^3J_{55\text{-}54}$ = 7.8 Hz, $^3J_{2\text{-}1}$ = $^3J_{55\text{-}56}$ = 5.3 Hz, H2, H55), 7.38 (dd, $^3J_{3\text{-}4}$ = $^3J_{54\text{-}53}$ = 7.8 Hz, $^3J_{3\text{-}2}$ = $^3J_{54\text{-}55}$ = 7.8 Hz, H3, H54), 7.29 (d, $^3J_{15\text{-}14}$ = $^3J_{42\text{-}43}$ = 4.7 Hz, H15, H42), 7.21 (dd, $^3J_{8\text{-}7}$ = $^3J_{49\text{-}50}$ = 8.0 Hz, $^3J_{8\text{-}9}$ = $^3J_{49\text{-}48}$ = 7.6 Hz, H8, H49), 7.20 (dd, $^3J_{14\text{-}13}$ = $^3J_{43\text{-}44}$ = 7.8 Hz, $^3J_{14\text{-}15}$ = $^3J_{43\text{-}42}$ = 4.7 Hz, H14, H43). NMR is assigned following the labels in Figure 2. MALDI-MS (CH$_2$Cl$_2$): m/z = 592.2 ([Ru(Cl)(Hbpp)(trpy)]$^+$). Cyclic Voltammetry (CH$_2$Cl$_2$, TBAH): E$_{1/2}$ = 0.669 V *vs.* SSCE (ΔE = 185 mV).

***out,out*-{[Ru(trpy)(H$_2$O)]$_2$(μ-[Zn(bpp)$_2$])}(ClO$_4$)$_4$,·(CH$_3$)$_2$CO, *out*-4·(CH$_3$)$_2$CO.** A 50 mg (0.033 mmol) sample of *out,out*-{[Ru(Cl)(trpy)]$_2$(μ-[Zn(bpp)$_2$])}(PF$_6$)$_2$ were placed in a 5 mL round bottom flask together with a 13.3 mg (0.064 mmol) of AgClO$_4$. The solids were dissolved with 10 mL of a 1:3 water/acetone solution (v/v) and refluxed for 1.5 h in the dark. The solution was then cooled in an ice bath and filtered over Celite to remove precipitated AgCl. A few drops of a saturated aqueous NaClO$_4$ solution was added to the filtrate, and the volume reduced under vacuum, keeping the temperature below 30 °C, until a precipitate appeared. The precipitation was completed by immersion in an ice bath for 30 minutes and the solid obtained filtered through a frit, washed with cold water (3 x 10 mL) and ether (3 x 10 mL), and dried in a vacuum.

5

Yield: 49 mg (92.9%). Anal. Calcd for $C_{56}H_{44}Cl_4N_{14}O_{18}Ru_2Zn\cdot(CH_3)_2CO$: C, 42.47; H, 3.02; N, 11.75. Found: C, 42.16; H, 3.16; N, 11.65. MALDI-MS (H_2O): m/z = 556.2 ([Ru(bpp)(trpy)]$^+$), 598.6 ([Ru(bpp)(trpy)(OH)(Na)]$^+$).

in,in-{[Ru(Cl)(trpy)]$_2$(µ-[Zn(bpp)$_2$])}(PF$_6$)$_2$, in-3. ROUTE A. A 100 mg (0.132 mmol) sample of *in*-[Ru(Cl)(Hbpp)(trpy)](PF$_6$) was dissolved in 40 mL of methanol, and then 19.0 mL of triethylamine (0.136 mmol) was slowly added to the solution under magnetic stirring and heating at 50 ºC. Afterwards, 90 mg of ZnCl$_2$ (0.660 mmol) previously dissolved in 10 mL of methanol was added, and the solution was kept stirring for 1 h at 50 ºC. The solvent was evaporated and the red solid dissolved in acetone. Some drops of a saturated KPF$_6$ aqueous solution and water were added and the volume reduced until the formation of a precipitate. The mixture was then left in a fridge overnight to complete precipitation, then filtered and washed with water (3 x 10 mL) and ether (3 x 10 mL). Yield: 87 mg (85.7%). Anal. Calcd for $C_{56}H_{40}Cl_2F_{12}N_{14}P_2Ru_2Zn\cdot2.8(KPF_6)$: C, 32.52; H, 1.95; N, 9.48. Found: C, 32.99; H, 2.01; N, 9.15. Cyclic Voltammetry (CH$_2$Cl$_2$, TBAH): $E_{1/2}$ = 0.665 V *vs.* SSCE (ΔE = 68 mV), $E_{1/2}$ = 0.765 V vs SSCE (ΔE = 66 mV). ^{1}H NMR (400 MHz, d_6-acetone): δ = 8.69 (d, $^3J_{7\text{-}8}$ = $^3J_{50\text{-}49}$ = 7.9 Hz, H7, H50), 8.67 (d, $^3J_{9\text{-}8}$ = $^3J_{48\text{-}49}$ = 8.0 Hz, H9, H48), 8.57 (d, $^3J_{12\text{-}13}$ = $^3J_{45\text{-}44}$ = 5.0 Hz, H12, H45), 8.53 (d, $^3J_{28\text{-}27}$ = $^3J_{29\text{-}30}$ = 7.9 Hz, H28, H29), 8.40 (d, $^3J_{4\text{-}3}$ = $^3J_{53\text{-}54}$ = 7.9 Hz, H4, H53), 8.18 (m, H15, H42), 8.17 (d, $^3J_{19\text{-}18}$ = $^3J_{38\text{-}39}$ = 8.4 Hz, H19, H38), 8.14 (dd, $^3J_{8\text{-}9}$ = $^3J_{49\text{-}48}$ = 8.0 Hz, $^3J_{8\text{-}7}$ = $^3J_{49\text{-}50}$ = 7.9 Hz, H8, H49), 8.09 (m, H14, H43), 8.00 (d, $^3J_{25\text{-}26}$ = $^3J_{32\text{-}31}$ = 6.9 Hz, H25, H32), 7.99 (s, H22, H35), 7.94 (dd, $^3J_{27\text{-}28}$ = $^3J_{30\text{-}29}$ = 7.9 Hz, $^3J_{27\text{-}26}$ = $^3J_{30\text{-}31}$ = 7.0 Hz, H27, H30), 7.77 (d, $^3J_{1\text{-}2}$ = $^3J_{56\text{-}55}$ = 5.7 Hz, H1, H56), 7.65 (dd, $^3J_{3\text{-}4}$ = $^3J_{54\text{-}53}$ = 7.9 Hz, $^3J_{3\text{-}2}$ = $^3J_{54\text{-}55}$ = 7.7 Hz, H3, H54), 7.60 (dd, $^3J_{18\text{-}19}$ = $^3J_{39\text{-}38}$ = 8.4, $^3J_{18\text{-}17}$ = $^3J_{39\text{-}40}$ = 7.5 Hz, H18, H39), 7.59 (dd, $^3J_{26\text{-}27}$ = $^3J_{31\text{-}30}$ = 7.0 Hz, $^3J_{26\text{-}25}$ = $^3J_{31\text{-}32}$ = 6.9 Hz, H26, H31), 7.42 (dd, $^3J_{13\text{-}14}$ = $^3J_{44\text{-}43}$ = 6.9 Hz, $^3J_{13\text{-}12}$ = $^3J_{44\text{-}45}$ = 5.0 Hz, H13, H44), 7.10 (d, $^3J_{16\text{-}17}$ = $^3J_{41\text{-}40}$ = 6.4 Hz, H16, H41), 6.76 (dd, $^3J_{17\text{-}18}$ = $^3J_{40\text{-}39}$ = 7.5 Hz, $^3J_{17\text{-}16}$ = $^3J_{40\text{-}41}$ = 6.4 Hz, H17, H40), 6.42 (dd, $^3J_{2\text{-}3}$ = $^3J_{55\text{-}54}$ = 7.7 Hz, $^3J_{2\text{-}1}$ = $^3J_{55\text{-}56}$ = 5.7 Hz, H2, H55). NMR is assigned following the labels in Figure 2. MALDI-MS (CH$_2$Cl$_2$): m/z = 1391.2 ([M-PF$_6$]$^+$).

ROUTE B. A 150 mg (0.098 mmol) sample of *out,out*-{[Ru(Cl)(trpy)]$_2$(µ-[Zn(bpp)$_2$])}(PF$_6$)$_2$ was dissolved in 130 mL of acetone and refluxed in presence of a 100 W lamp for 72 hours. Then a few drops of a saturated KPF$_6$ aqueous solution and

water were added and the volume reduced until the formation of a precipitate. The mixture was left in a fridge overnight to complete precipitation, then filtered and washed with water (3 x 10 mL) and ether (3 x 10 mL).

Yield: 128 mg (85.3 %).

in,in-{[Ru^{III}(trpy)]$_2$(μ-[Zn(bpp)$_2$(H$_2$O)]μ-(O)}(ClO$_4$)]$_4$, in-5. A 50 mg (0.033 mmol) sample of in,in-{[Ru(Cl)(trpy)]$_2$(μ-[Zn(bpp)$_2$])}(PF$_6$)$_2$ were placed in a 5 mL round bottom flask together with a 13.3 mg (0.064 mmol) of AgClO$_4$. The solids were dissolved with 10 mL of a 1:3 water/acetone solution (v/v) and refluxed for 1.5 h in the dark. The solution was then cooled in an ice bath and filtered over Celite to remove precipitated AgCl. A few drops of a saturated aqueous NaClO$_4$ solution was added to the filtrate, and the volume reduced under vacuum, keeping the temperature below 30 °C, until a precipitate appeared. The precipitation was completed by immersion in an ice bath for 30 minutes and the solid obtained filtered through a frit, washed with cold water (3 x 10 mL) and ether (3 x 10 mL), and dried in a vacuum. Yield: 11 mg (19.5 %). Anal. Calcd for C$_{56}$H$_{42}$Cl$_4$N$_{14}$O$_{18}$Ru$_2$Zn·2(LiClO$_4$)·(CH$_3$)$_2$CO: C, 37.71; H, 2.57; N, 10.43. Found: C, 37.98; H, 2.40; N, 10.64. MALDI-MS (CH$_2$Cl$_2$): m/z = 656.2 ([Ru(bpp)(trpy)](ClO$_4$)$^+$). Cyclic Voltammetry (H$_2$O, pH = 1.0 CF$_3$SO$_3$H): $E_{1/2}$ = 0.310 V vs SSCE (ΔE = 93 mV), $E_{1/2}$ = 0.730 V vs SSCE (ΔE = 81 mV); (H$_2$O, pH = 7.0 phosphate buffer): $E_{1/2}$ = 0.152 V vs SSCE (ΔE = 204 mV), $E_{1/2}$ = 0.780 V vs SSCE (ΔE = 101 mV).

X-ray Crystal Structure Determination. Black crystals of *out*-{[Ru(Cl)(trpy)][ZnCl$_2$](μ-bpp)}, **out-2**, were obtained by slow diffusion of acetone into a dimethyl formamide solution of the complex. Brown crystals of *out,out*-{[Ru(Cl)(trpy)]$_2$(μ-[Zn(bpp)$_2$])}(PF$_6$)$_2$, **out-3**, were obtained by slow diffusion of ether in a methanolic solution of the complex. Dark red crystals of *in,in*-{[Ru(Cl)(trpy)]$_2$(μ-[Zn(bpp)$_2$])}(PF$_6$)$_2$, **in-3**, could be obtained by slow diffusion of ether in a methanolic solution of the complex. Green crystals of *in,in*-{[Ru^{III}(trpy)]$_2\mu$-[Zn(bpp)$_2$(H$_2$O)]μ-(O)}(ClO$_4$)]$_4$, **in-5**, were obtained by slow diffusion of ether in acetone solution of the complex. The measured crystals were prepared under inert conditions immersed in perfluoropolyether as protecting oil for manipulation.

Data collection: Crystal structure determination for **out-2** was carried out using a Apex DUO Kappa 4-axis goniometer equipped with an APPEX 2 4K CCD area detector, a

7

Microfocus Source E025 IuS using MoK_α radiation, Quazar MX multilayer Optics as monochromator and a Oxford Cryosystems low temperature device Cryostream 700 plus ($T = -173$ °C). Full-sphere data collection was used with ω and φ scans. *Programs used:* Data collection APEX-2,[13] data reduction Bruker Saint[14] V/.60A and absorption correction SADABS.[1516] Crystal structure determinations for *out*-3, *in*-3 and *in*-5 were carried out using a Bruker-Nonius diffractometer equipped with an APPEX 2 4K CCD area detector, a FR591 rotating anode with MoK_α radiation, Montel mirrors as monochromator and an Oxford Cryosystems low temperature device Cryostream 700 plus ($T = -173$ °C).

Structure Solution and Refinement: Crystal structure solution was achieved using direct methods as implemented in SHELXTL[17] and visualized using the program XP. Missing atoms were subsequently located from difference Fourier synthesis and added to the atom list. Least-squares refinement on F^2 using all measured intensities was carried out using the program SHELXTL. All non hydrogen atoms were refined including anisotropic displacement parameters.

Comments to the structures: *out*-2: The asymmetric unit contains two independent molecules of the bimetallic complex, three DMF molecules and three water molecules. One of the DMF molecules and one of the water molecules are disordered in two positions (ratio respectively: 75:25 and 50:50). Due to the disorder of the water molecules the positions of the corresponding hydrogen atoms could not be clearly localized and these were added to approximate positions to satisfy the crystal stoichiometry. This disorder is thus responsible for the B alerts that appear in the checkcif file. *out*-3: The asymmetric unit contains two independent molecules of the metallic complex, four PF_6 anions and 4.6 water molecules which are highly disordered distributed in 7 positions (1:1:0.6:0.6:0.6:0.4:0.4). As in the previous case hydrogen atoms could not be clearly localized and were added at approximate. *in*-3: The asymmetric unit contains one molecules of the metallic complex, two PF_6 anions, one acetone molecule and one methanol molecule. One of the PF_6 anions is disordered in two orientations (ratio: 80:20). The methanol molecule is disordered in three positions (ratio: 62.5:25:12.5). *in*-5: The asymmetric unit contains one molecule of the metallic complex, four ClO_4 anions and one and half nonmetal coordinated water molecules. Three of the ClO_4 anions are disordered in two orientations (ratios: 60:40; 36:74;
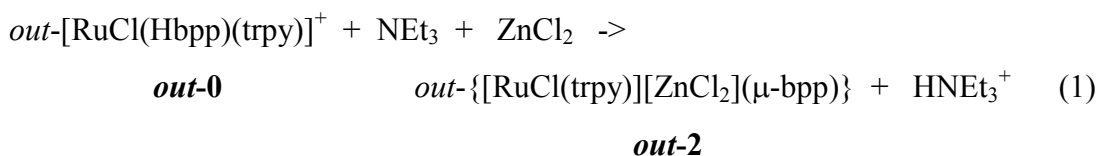
81:19). The one and half nonmetal coordinated water molecules are disordered in three positions (ratio: 65:35:50).

Computational details: All calculations were carried out by using the Amsterdam Density Functional (ADF v2013.01) package.[18] DFT-based methods employed the generalized-gradient-approximation (GGA) level, with the Becke exchange[19] and the Perdew correlation[20] functionals (BP86). A triple-ξ plus polarization Slater basis set was used on all atoms. Relativistic corrections were introduced by scalar-relativistic zero-order regular approximation (ZORA).[21] Full geometry optimizations were performed without constraints, and also including Grimme's DFT-D empirical dispersion energy corrections.[22]

Results and Discussion

Synthesis and structure. The non-symmetric dinucleating nature of Hbpp ligand[23] allows for the easy preparation of heteronuclear complexes given the different reactivity of the two available sites. Initially mononuclear complexes can be prepared leaving the second site ready for a second transition metal to coordinate. In the present report we have used the mononuclear isomeric complexes *in-* and *out-*[RuCl(Hbpp)(trpy)]$^+$, ***in-*0** and ***out-*0**[11a] as starting materials following the synthetic strategy described in Scheme 1.

Reaction of *out-*[RuCl(Hbpp)(trpy)]$^+$, ***out-*0**, with excess of $ZnCl_2$ in presence of triethylamine, that acts as a base, in methanol at 50 ºC for 1 hour produces the complex *out-*{[Ru(Cl)(trpy)][ZnCl$_2$](μ-bpp)}, ***out-*2**, almost quantitatively.

$$\textit{out-}[RuCl(Hbpp)(trpy)]^+ \ + \ NEt_3 \ + \ ZnCl_2 \ ->$$

$$\textbf{\textit{out-}0} \qquad\qquad \textit{out-}\{[RuCl(trpy)][ZnCl_2](\mu\text{-bpp})\} \ + \ HNEt_3^+ \quad (1)$$
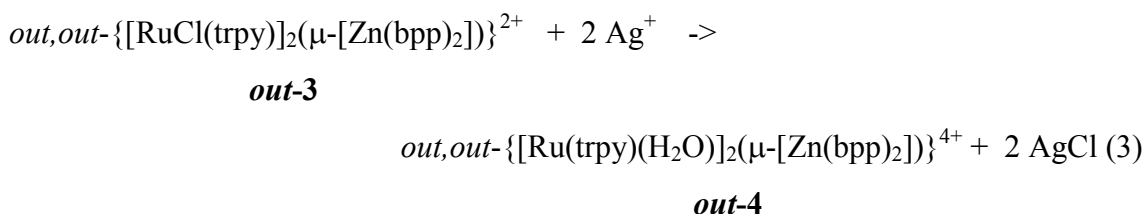
$$\textbf{\textit{out-}2}$$

Complex ***out-*2** precipitates readily from the methanolic solution and is insoluble in water and in most organic solvents except in DCM, DMSO and DMF. Dissolved in the

9

latter the complex has a strong tendency to dimerize generating a heterotrinuclear complex, according to,
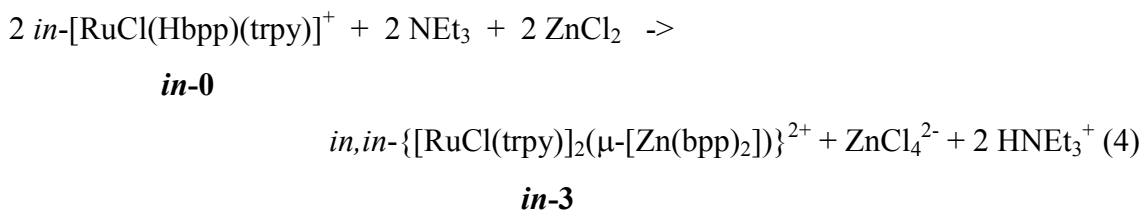
2 out-{[RuCl(trpy)][ZnCl$_2$](μ-bpp)} ->
$$\textbf{\textit{out-2}} \qquad\qquad out,out\text{-}\{[\text{RuCl(trpy)}]_2(\mu\text{-}[\text{Zn(bpp)}_2])\}^{2+} + \text{ZnCl}_4^{2-} \quad (2)$$
$$\textbf{\textit{out-3}}$$
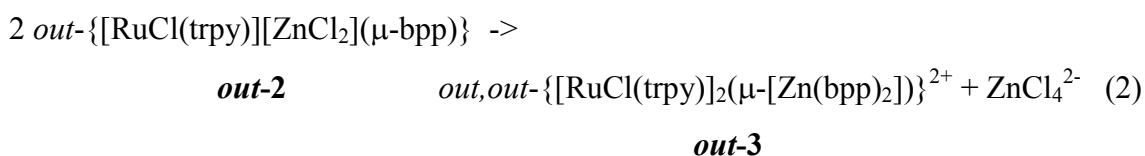
where the Zn metal is now bonded to two bpp$^-$ ligands in an tetrahedral fashion and acts as bridged for the two [RuCl(trpy)] moieties. Addition of Ag(I) to $\textbf{\textit{out-3}}$ generates the corresponding Ru diaqua complex,

$$out,out\text{-}\{[\text{RuCl(trpy)}]_2(\mu\text{-}[\text{Zn(bpp)}_2])\}^{2+} \;+\; 2\,\text{Ag}^+ \;\to$$
$$\textbf{\textit{out-3}}$$
$$out,out\text{-}\{[\text{Ru(trpy)(H}_2\text{O)}]_2(\mu\text{-}[\text{Zn(bpp)}_2])\}^{4+} + \; 2\,\text{AgCl} \;(3)$$
$$\textbf{\textit{out-4}}$$

It is interesting to realize here that the yield for this reaction is nearly quantitative (93 %) in sharp contrast to the yield obtained for the formation the aqua complex $\textbf{\textit{out-1}}$ from $\textbf{\textit{out-0}}$ of 53%, under comparable conditions. This is a consequence of the potential coordination of Ag to the available coordination position of the bpp$^-$ ligand in $\textbf{\textit{out-0}}$ that can drive the systems to additional undesired pathways thus lowering the yield. In the present case the Zn metal avoids the interaction of silver with the bpp$^-$ ligands and thus is responsible for this large enhancement of the yield.

The parallel chemistry with the in isomer in-[RuCl(Hbpp)(trpy)]$^+$, $\textbf{\textit{in-0}}$, is radically different from the previously described reactions. In this case the addition of ZnCl$_2$ generates directly the heterotrinuclear complex,

2 in-[RuCl(Hbpp)(trpy)]$^+$ + 2 NEt$_3$ + 2 ZnCl$_2$ ->
$$\textbf{\textit{in-0}}$$
$$in,in\text{-}\{[\text{RuCl(trpy)}]_2(\mu\text{-}[\text{Zn(bpp)}_2])\}^{2+} + \text{ZnCl}_4^{2-} + 2\,\text{HNEt}_3^+ \;(4)$$
$$\textbf{\textit{in-3}}$$

10

presumably due to the solubility of the corresponding *in-2* dinuclear isomer that could not be isolated. Addition of Ag(I) to *in-3* generates the corresponding diqua complex *in-4*, that again could not be isolated because it has a strong tendency to generate the oxo-bridged derivative, *in-5*,

$$in,in\text{-}\{[Ru^{II}(trpy)(H_2O)]_2(\mu\text{-}[Zn(bpp)_2])\}^{4+} \ \text{->}$$
$$in\text{-}4$$
$$in,in\text{-}\{[Ru^{III}(trpy)]_2(\mu\text{-}[Zn(bpp)_2(H_2O)]\mu\text{-}(O)\}^{4+} + 2H^+ + 2e^- \quad (5)$$
$$in\text{-}5$$
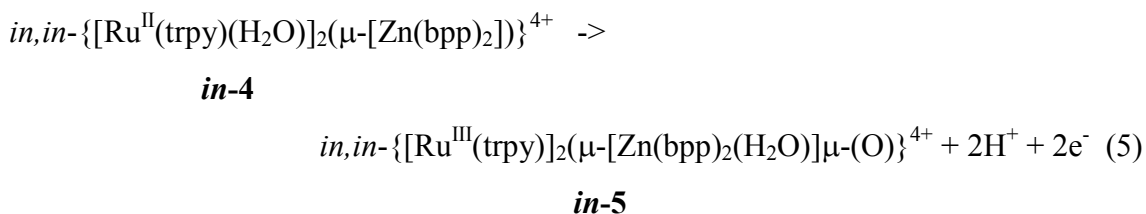
This is a consequence of the ligand architecture that in the case of the *in-4* complex places the two Ru-aqua groups very close to one another and favors the intramolecular [Ru-OH$_2$ --- H$_2$O-Ru] coupling, to generate the highly stable oxo bridge group, Ru-O-Ru concomitant with the oxidation of Ru(II) to Ru(III) doubly bridging the Ru centers. The formation of this group is also most likely responsible for the five coordination of the Zn complex with an additional aqua group. Given the absence of crystal field stabilization energy for a d^{10} ion, the new structural demands imposed by the oxo-bridging group forces a distortion of the N4 coordination by the bpp$^-$ ligands favoring a pentacoordinate geometry with an additional Ru-O bond from the aquo ligand. See below for further details of the coordination geometry of the Zn metal ion.

Monocrystals for complexes *out-2*, *out-3*, *in-3* and *in-5* were obtained and their crystal structures were solved by means of x-ray diffraction analysis. Their Ortep view is presented in Figure 1, and all the crystallographic parameters can be found in the SI as cif files. For all these complexes the coordination around the low spin d^6 Ru(II) or d^5 Ru(III) is a distorted octahedral and very similar to previously reported related Ru complexes.[10a, 11b, 24] In sharp contrast, while the bonding distances for the Zn(II) are also in agreement with previously published related complexes,[25] their geometries are radically different from one another. This is a consequence of the absence of Crystal Field Stabilization Energy (CFSE) for a d^{10} Zn(II) ion where the Zn metal center geometry is strongly dependent on the spatial effects exerted by the coordinating bridging bpp$^-$ ligand, that are in turn dependent on their geometrical arrangement around the Ru metal center.

11

For the **out-2** heterodinuclear complex, the Zn center is a coordinated by two Cl and two N-atoms from the bpp⁻ ligands in a distorted tetrahedral fashion. The dihedral angle between the planes generated by the Cl2Zn1Cl3 atoms and the N6Zn1N7 is 86.4°, close to the 90° expected for an ideal tetrahedral geometry. For the **out-3** heterotrinuclear complex, the geometry around the Zn metal center is again a distorted tetrahedron although now the coordination atoms are two N atoms from a pyridyl-pyrazolyl moiety from two different bpp⁻ ligands. The dihedral angle between the two NZnN (N6Zn1N7 and N8Zn1N9) planes is now 78.2°. It is worth noting here that the trpy an bpp⁻ moieties bonded to different Ru centers, are situated in a nearly parallel manner although they are too far for a potential π- π stacking interaction.

Regarding the **in-3** complex, the constitutional isomer of **out-3**, the geometry presented by Zn is now closer to a distorted octahedral geometry, where due to the new spatial arrangement of the Ru-Cl-Hbpp moiety, their Cl atoms weakly interact with the Zn metal (d_{Zn-Cl} = 3.06 and 3.04 Å respectively). In this case the NZnN (N6Zn1N7 and N8Zn1N9) dihedral angle is 85.9°. Finally for the **in-5** complex, that contains a Ru-O-Ru group, the Zn metal displays penta-coordination with an additional Zn-OH$_2$ group in a distorted square pyramidal type of geometry. Here the NZnN (N6Zn1N7 and N8Zn1N9) dihedral angle is 47.9°, which is the smallest of all the complexes described in the present work due to the special arrangement forced by the additional oxo-bridging group between the two Ru(III) centers. It is also worth mentioning here that the oxygen atom of the Zn-OH$_2$ groups is hydrogen bonded to a H56, of one of the trpy ligands (C56H56O2 angle 146.6°; C56O2, 3.43 Å; H56O2, 2.60 Å).

Spectroscopic proprieties. The optical properties of the Ru-Cl complexes presented in this work were evaluated by means of UV-vis spectroscopy in DCM and are displayed in Figure 3. All complexes present strong ligand based π-π* bands below 340 nm and lower intensity MLCT dπ-π* transitions around 400 and 700 nm together with their vibronic components.[26] TDFT has been used to corroborate the nature of these transition and the results are shown in the supporting information (Figure S16).
The spectra of all the complexes are very similar since the chromophores are identical. As expected, the presence in the system of a d^0 metal, such as Zn(II), doesn't significantly modify the overall optical properties in the visible region. A slight

12

difference can be found from *in-* an *out-***3** on energies and extinction coefficients that might be due to the slightly geometrical distortions found in the Ru metal centers. Similar behavior is observed for the *in* complexes (Fig 2, right), where the interaction between the chlorido ligands and the Zinc atom seems to produce a small shift of the dπ-π* MLCT band to higher energy.

The *in-***5** complex was investigated in aqueous solution. At pH 1.0, it presents the typical bands of the Ru-O-Ru transition at 610 and 680 nm as can be observed in Figure 4. These two bands are red-shifted by about 50 nm at pH 7.0 which is indicative of the acid base properties of the oxo-bridge as had been previously observed for related oxo-bridged-Ru dimers.[27]

Fluorescence experiments have been carried out for the complexes *out-***2***, out-***3 and *in-***3,** and for their mononuclear analogues *out-***0 and *in-***0** for comparison purposes. All these spectra are presented as insets in Figure 3. From the figure it can be clearly seen that the emission is affected by the nature of the monodentate ligand but is practically not affected by the nature of the isomer.

Redox proprieties. The redox properties of the Ru-Cl complexes presented in this work were analyzed by means of cyclic voltammetry in DCM containing 0.1 M TBAH [(nBu$_4$N)(PF$_6$)] as supporting electrolyte, and are displayed in Figure 5. All redox potentials reported in this work are referred to the SSCE electrode and all CV were run at a scan rate of 50 mV/s. Glassy carbon electrodes were used as working electrodes and platinum wire as auxiliary electrodes.

The dinuclear complex *out-***2** exhibits a chemically reversible and electochemically quasi-reversible wave at $E_{1/2} = 0.54$ V ($\Delta E_{a,p} = 76$ mV), assigned to the Ru(III)/Ru(II) couple, which is 80 mV lower than *out-***0** ($E_{1/2} = 0.62$ V) under identical conditions. Thus the replacement of the pyrazolic-Hbpp proton by the ZnCl$_2$ group produces an enhancement of the electron density on the Ru metal center. The trinuclear complex *out-***3** shows two waves in very close proximity at $E_{1/2} = 0.64$ V ($\Delta E = 120$ mV) and $E_{1/2} = 0.695$ V ($\Delta E = 150$ mV), assigned to the Ru$_2$(III,II)/Ru$_2$(II/II) and Ru$_2$(III,III)/Ru$_2$(III/II) couples respectively. The close proximity of the two couples suggests a weak electronic coupling between the two Ru centers through the {Zn(bpp)$_2$} bridging unit, as expected.[10a, 28] Comparing the redox potential for the mononuclear *out-***0** with regard to *out-***3** a decrease of electron density over the Ru metal centers is now observed as suggested by the anodic shift of the III/II redox potentials.

13

In the case of **in-3**, two quasi-reversible waves at $E_{1/2} = 0.66$ V ($\Delta E = 80$ mV) and $E_{1/2} = 0.76$ V ($\Delta E = 80$ mV) assigned to the $Ru_2(III,II)/Ru_2(II/II)$ and $Ru_2(III,III)/Ru_2(III/II)$ couples respectively, indicate again a weak coupling but now the two waves are cathodically shifted by 80-180 mV with regard to **in-0** ($E_{1/2} = 0.84$ V). This effect can be associated with the Zn-Cl contacts (3.04 and 3.06 A) that each {Ru-Cl} entity has in the *in* isomer and that do not exist in the corresponding *out* isomer. These Zn-Cl contacts that generate the difference in redox potentials are also most likely responsible for the difference in the weak electronic coupling through the two Ru metals. NIR experiments for the mixed valence III,II **in-3** complex were carried out in order to further characterized the electronic coupling. Unfortunately the IVCT band is so weak[29] that we were not able to properly observe it (see Figure S14-15) even working at the highest possible concentration.

The oxo-bridged complex **in-5** presents a completely different redox behavior. In water at pH = 1.0 a reversible wave at $E_{1/2} = 0.84$ V ($E_{p,a} = 0.87$ V, $E_{p,c} = 0.81$ V; $\Delta E = 60$ mV) associated with the $Ru_2(IV,III)/Ru_2(III/III)$ couple is observed as can be observed in Figure 4. In addition a chemically irreversible wave is observed at 0.25 V that is associated with the one electron reduction of the oxo-bridged trinuclear complex to generate $Ru_2(III/II)$. The chemical irreversibility is associated with the instability of the Ru-O-Ru bridged in the lower oxidation state where the population of antibonding orbitals[27] favors the breaking of the bridging group generating the corresponding mononuclear complexes.

NMR Spectroscopy. ^{1}H-NMR spectra of the complexes described in this work were recorded in d_6-dmso or d_6-acetone and are assigned in the Experimental Section and their spectra are shown in Figure 2 and in the SI.

In solution complex **out-2** presents a symmetry plane that contains the bpp⁻ ligand and bisects the trpy moiety, thus rendering the upper and lower pyridyl of the trpy ligand magnetically equivalent. The deshielding effect produced by the Cl ligand at H16 allows one to identify the pyridyl system on the side of the Ru center. This information, together with the COSY spectra and symmetry of the complex previously mentioned, allow to unambiguously assigning all the resonances of the spectra (See Figure S1 in SI).

14

The ^{1}H-NMR spectra of complexes **out-3** and **in-3** in d$_6$-acetone is depicted in Figure 2. Both exhibit a C_2 symmetry axis passing through the Zn atom but not coinciding with any bond and thus in both cases the two {Ru-Hbpp-trpy} moieties are magnetically equivalent. Symmetry, together with COSY and the deshielding effect of the chloro ligands to H16 and H41 for the **out-3** complex, allow fully identifying all resonances. For the case of the **in-3,** a NOE between H14 and H29 (2.80 Å) or H28 and H42 (2.78 Å) is the key experiment that allows fully assigning the spectrum shown in Figure 2.

Reactivity. In both neutral and acidic conditions the trinuclear **out-4** Ru-aqua complex breaks apart and generates the corresponding mononuclear complex **out-1**, as indicated in the following equation,

$$out,out\text{-}\{[Ru^{II}(trpy)(H_2O)]_2(\mu\text{-}[Zn(bpp)_2])\}^{4+} \ + \ 2\,H_2O \ \rightarrow$$
$$\textbf{\textit{out-4}}$$

$$2\ out\text{-}[Ru^{II}(Hbpp)(trpy)(H_2O)]^{2+} \ + Zn(OH)_2 \ \ (6)$$
$$\textbf{\textit{out-1}}$$
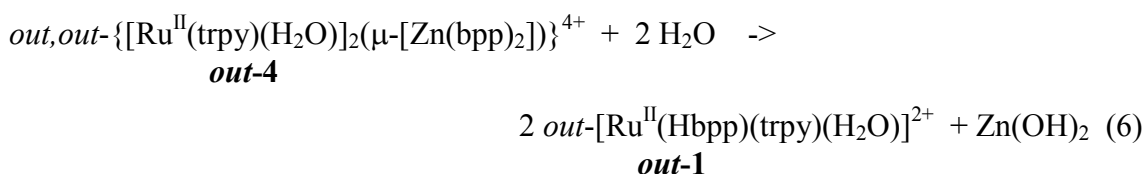
The generation of the mononuclear complex is instantaneous once the trinuclear complex is dissolved in aqueous solution as can be clearly observed by UV-vis and CV.

On the other hand the trinuclear **out-3** complex is photosensible and under irradiation with a tungsten lamp, cleanly and irreversibly and quantitatively isomerizes to **in-3.** This isomerization process has been monitored by ^{1}H-NMR spectroscopy and is shown in Figure 2. This is in sharp contrast with the photostability of the synthetic precursors, the mononuclear **in-** and **out-1** complexes.

The irreversible isomerization of the complex **out-3** towards **in-3**, is a consequence of the higher thermodynamic stability of the latter over the former. In addition, even though experimentally we could not detect any intermediate, the transformation of the *out,out* complex into the *in,in* complex necessarily has to take place via the corresponding *in,out* intermediate complex, as indicated in the following equations (bpp and trpy ligands and overall charges have been omitted).

15

out,out-{[RuCl]$_2$(μ-Zn)} -> *in,out*-{[RuCl]$_2$(μ-Zn)} -> *in,in*-{[RuCl]$_2$(μ-Zn)} (7)

out-3   **_in,out_-3**   **_in_-3**
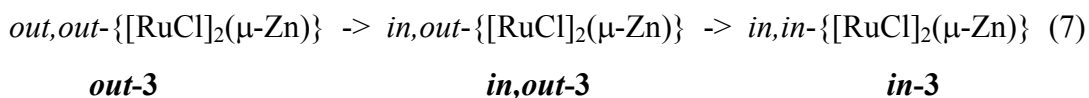
In order to shed light into the driving force for the isomerization process, a DFT based study was carried out and a summary of the main results is presented in Figure 6 and in the SI. For this purpose we determined the relative stability of isomers **_out_-3**, **_in,out_-3** and **_in_-3.** As it can be observed in Figure 6, the **_in,out_-3** complex is about 12.7 kcal/mol more stable than **_out_-3** mainly due to the formation of a new Zn-Cl bond (Zn-Cl, 2.621 Å). The isomerization of the second Ru center toward the formation of **_in_-3** is 13.8 kcal/mol more stable, now due to the two Zn-Cl contacts. This is actually a structure that is very close the one observed experimentally through the X-ray diffraction analysis that is represented in Figure 1. The Zn-Cl bond length obtained from the geometry optimization process (2.920; 2.877 Å) compares fairly well with the X-ray determined parameters (3.06; 3.04 Å) although is overestimated by approximately 0.1-0.2 Å. Including dispersion in the calculations further decrease the Zn-Cl distance by roughly 0.05 Å.

Conclusions

We have prepared and thoroughly characterized a family of dinuclear and trinuclear Zn-Ru complexes containing the bbp$^-$ ligand as a bridge. These include constitutional isomers that have been prepared from their corresponding *in* and *out* Ru mononuclear counterparts. The different constitutional isomers give rise not only to different solubilities but also to radically different reactivity based on the relative space disposition of the Ru-OH$_2$ or Ru-Cl groups. The access to through space intramolecular Ru-aqua---aqua-Ru interactions in **_in_-4** gives rise to the oxo-bridged complex. The oxo-bridge is holding strongly and rigidly together the two Ru centers and that enhances its stability so that now the trinuclear Ru complex is stable at pH 1.0 and 7.0 whereas the trinuclear *out* compelex is not. On the other hand for the Ru-Cl case the presence of contact interactions stabilize the *in* isomer with regard to the corresponding *out* one. The relative stability of the isomers is nicely demonstrated by the *out->in* photochemcial interconversion that is further supported by DFT.

The use of labile first row transition metals ion such as Zn, Fe or Mn to react with bridging dinucleating ligands such as Hbpp, generally produces oligomers[30] or grids[12a]

16

or even coordination polymers.[12b-d] Using a substitutionally kientically inert Ru(II) ion (at least with regard to the N-containing ligands) to coordinate first with the Hbpp ligand with the subsequent addition of a substitutionally kinetically labile ion such as Zn(II) precludes the potentials oligomerization process and thus allows to isolate the dinuclear and trinuclear complexes reported in the present work. As such these complexes can be considered as the corresponding synthetic intermediates used by first row transition metals to generate oligomers or coordination polymers.

Supporting Information content. Additional spectroscopic, electrochemical and DFT data. X-ray crystallographic data in CIF format (CCDC # 1014664-1014667). This material is available free of charge via the Internet at http://pubs.acs.org.

17

Scheme 1. Synthetic pathway.

Figure 1. X-Ray structure Ortep plots (probabilites at 50%) and labelling scheme for (A) *out*-**2**, (B) *out*-**3**, (C) *in*-**3** and (D) *in*-**5**.
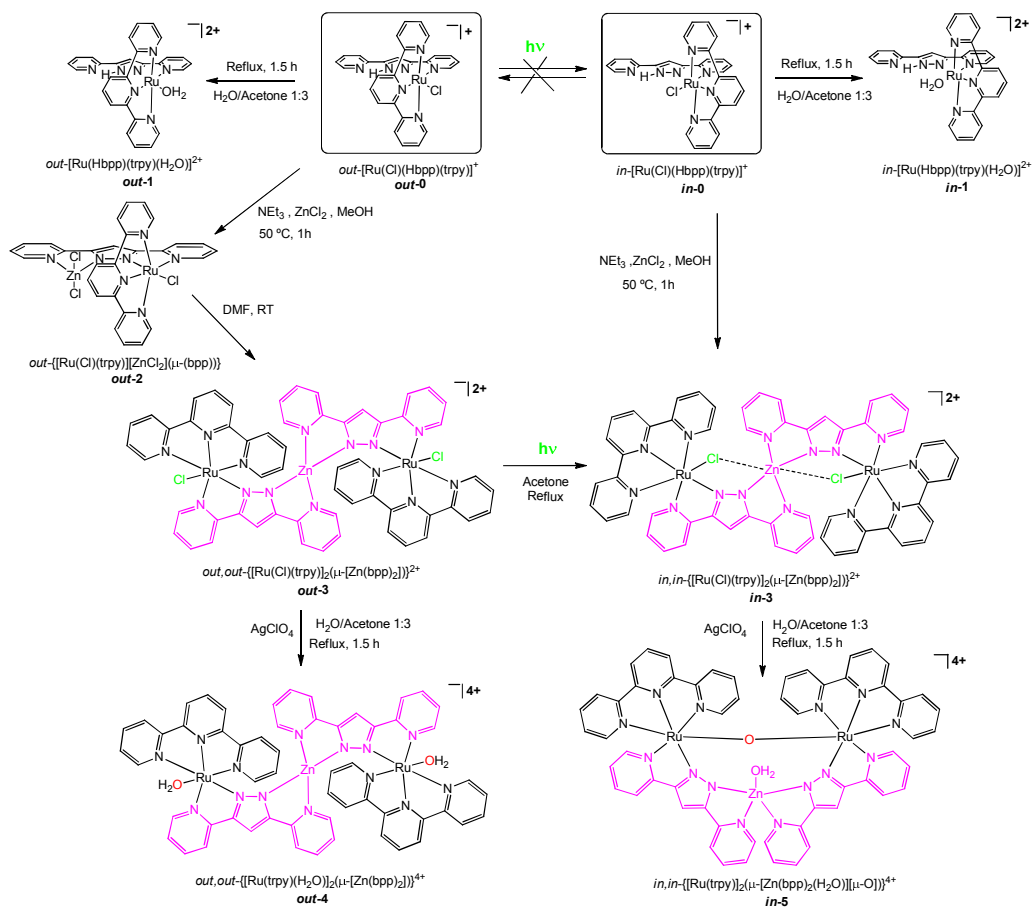
Figure 2. Top, ^{1}H-NMR spectra (400 MHz, 298 K, d$_6$-acetone) following the photochemical (100 W lamp) isomerization reaction from **out-3** to **in-3**. Bottom, time profile based on the integration of resonances H16 for **out-3** and H12+H28 for **in-3**.
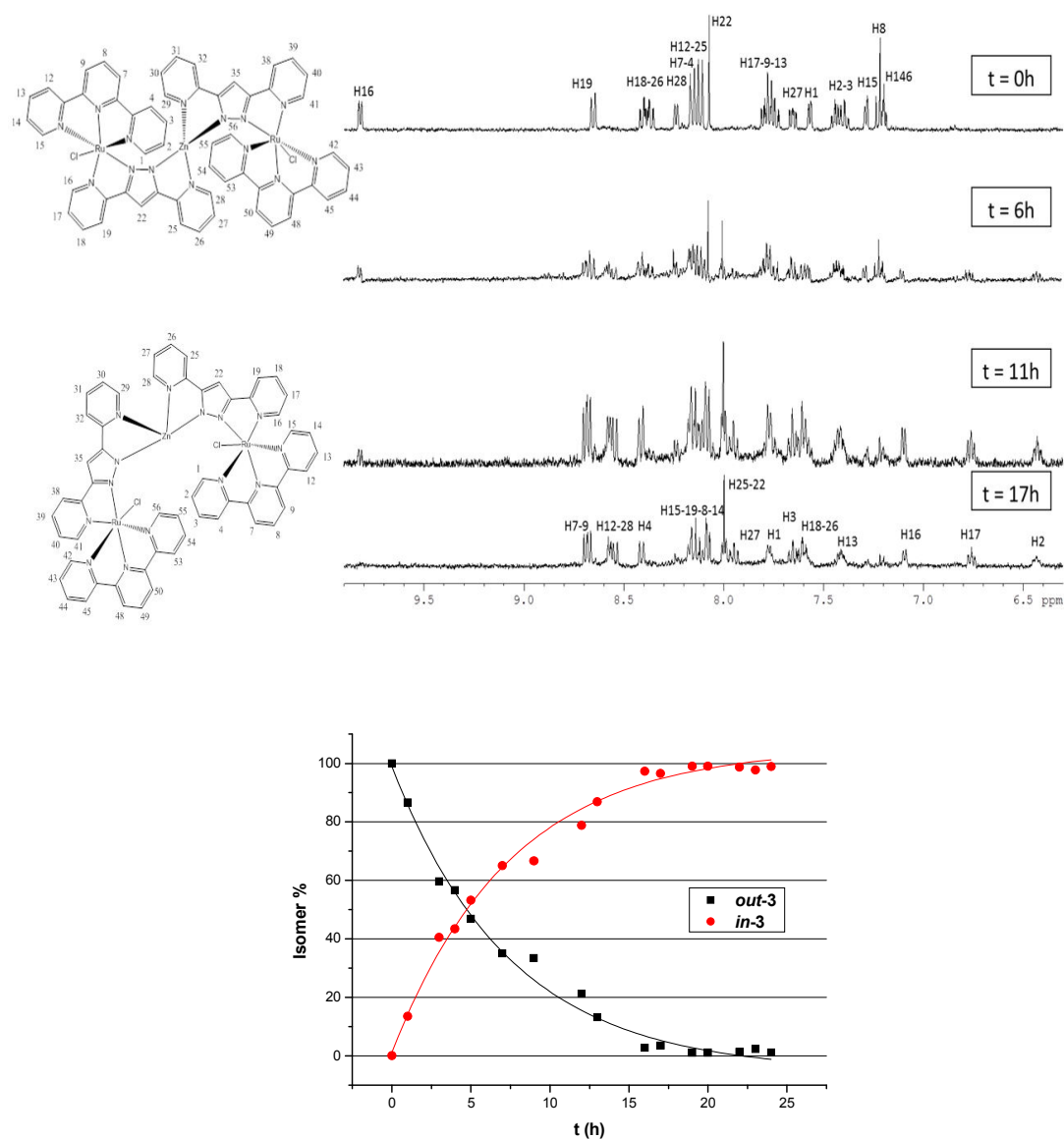
Figure 3. UV-vis and (inset) emission spectra in DCM of *out-***0**, *out-***2** and *out-***3** (left) and *in-***0,** *in-***3** and *out-***3** **(**right)**.**
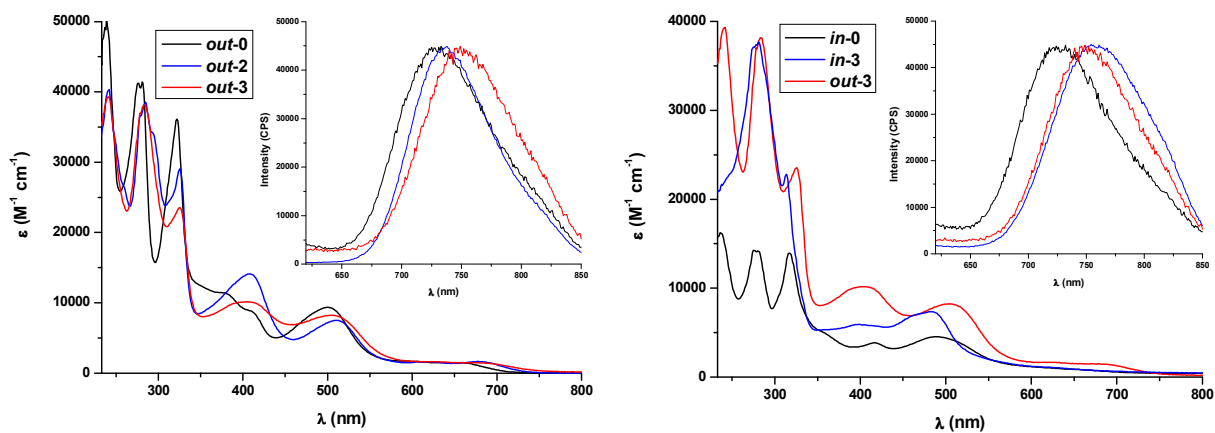
Figure 4. UV-vis at pH 1.0 and 7.0, and (inset) CV at pH 1.0 (E vs SCEE) of *in-***5**.
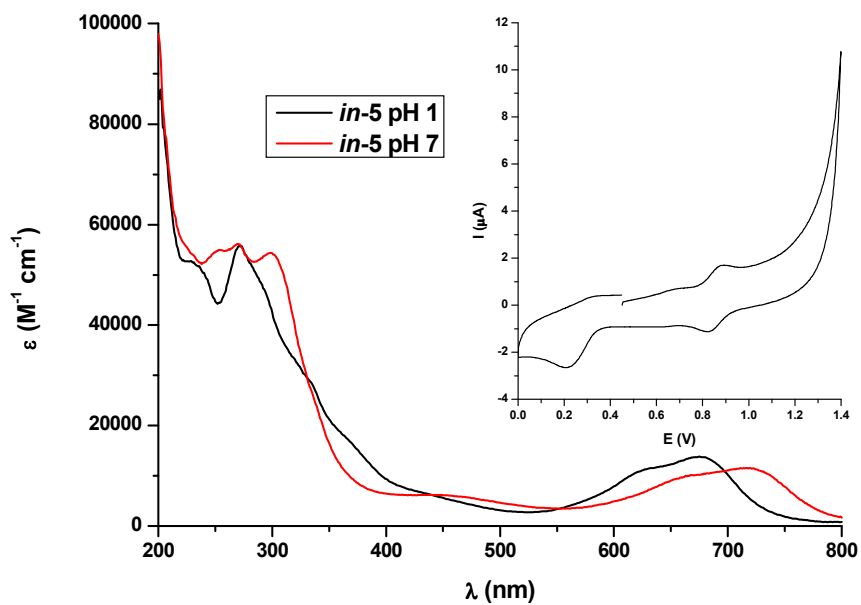
Figure 5. Cyclic voltammograms (E vs SCEE) in DCM containing 0.1 M TBAH [(*n*Bu₄N)(PF₆)] of: left, of **out-0**, **out-2** and **out-3** and right, cyclic voltammograms of **in-0** and **in-3** in DCM containing 0.1 M TBAH.
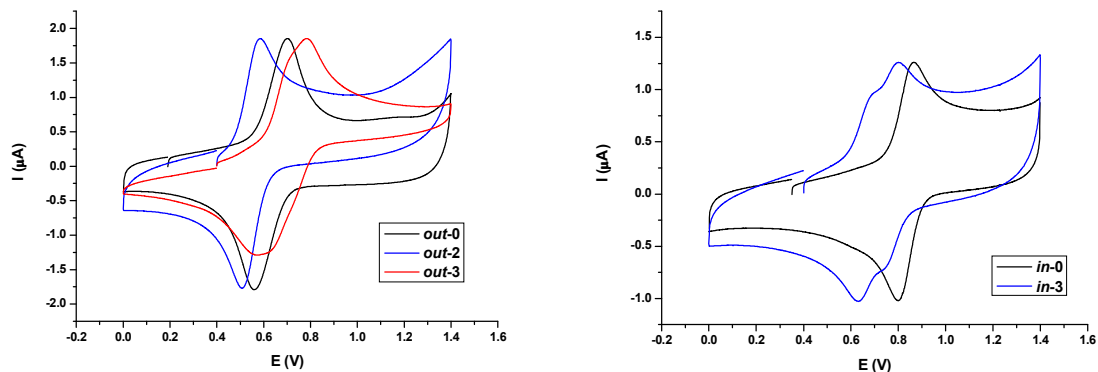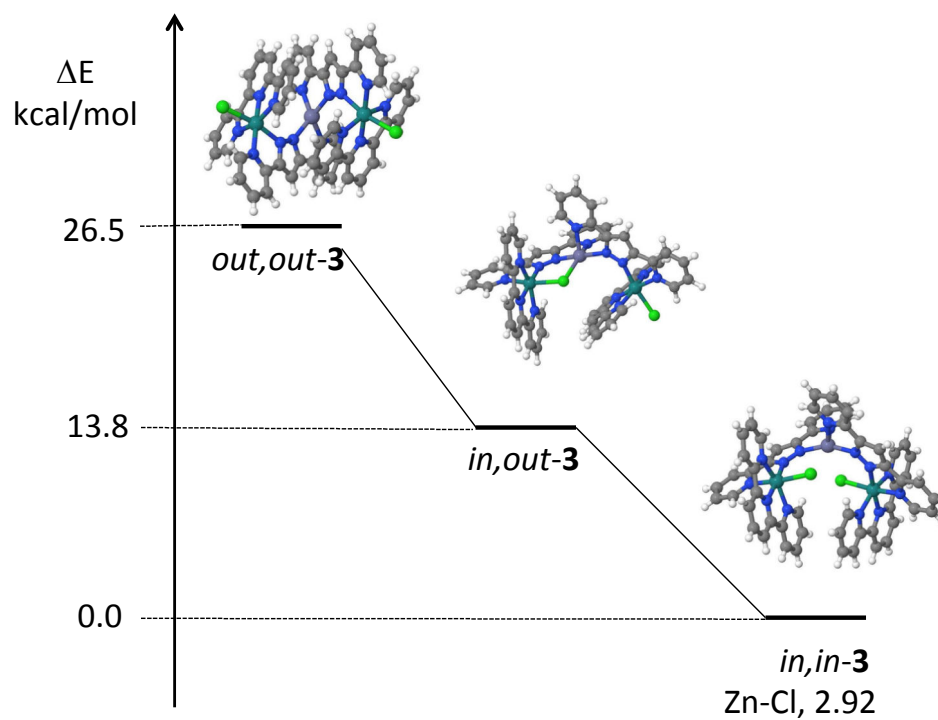

Figure 6. Energy diagram for optimized structures of three isomers of **3**, based on DFT.

REFERENCES

(1) a) Suzuki, M.; Furutachi, H.; Ōkawa, H. *Coord. Chem. Rev.* **2000,** *200–202*, 105-129; b) Gavrilova, A. L.; Bosnich, B. *Chem. Rev.* **2004,** *104*, 349-384; c) Gavrilova, A. L.; Qin, C. J.; Sommer, R. D.; Rheingold, A. L.; Bosnich, B. *J. Am. Chem. Soc.* **2002,** *124*, 1714-1722; d) Incarvito, C.; Rheingold, A. L.; Gavrilova, A. L.; Qin, C. J.; Bosnich, B. *Inorg. Chem.* **2001,** *40*, 4101-4108; e) García-Antón, J.; Bofill, R.; Escriche, L.; Llobet, A.; Sala, X. *Eur. J. Inorg. Chem.* **2012,** *2012*, 4775-4789; f) Halvagar, M. R.; Neisen, B.; Tolman, W. B. *Inorg. Chem.* **2012,** *52*, 793-799; g) Halvagar, M. R.; Tolman, W. B. *Inorg. Chem.* **2013,** *52*, 8306-8308; h) York, J. T.; Llobet, A.; Cramer, C. J.; Tolman, W. B. *J. Am. Chem. Soc.* **2007,** *129*, 7990-7999.

(2) a) Cornia, A.; Gatteschi, D.; Sessoli, R. *Coord. Chem. Rev.* **2001,** *219–221*, 573-604; b) Carlin, R. L., *Magnetochemistry*; Springer-Verlag: Berlin, 1986; c) Kahn, O., *Molecular Magnetism*; Wiley: 1993; d) Kahn, O., in *Modular Chemistry*, Michl, K. J., Ed. Kluwer Academic: Dordrecht, The Netherlands, 1997.

(3) Zhao, G.-J.; Han, K.-L. *Acc. Chem. Res.* **2011,** *45*, 404-413.

(4) a) Nieto, I.; Wooten, A. J.; Robinson, J. R.; Carroll, P. J.; Schelter, E. J.; Walsh, P. J. *Organometallics* **2013,** *32*, 7431-7439; b) Bratko, I.; Gomez, M. *Dalton Trans.* **2013,** *42*, 10664-10681.

(5) Neudeck, S.; Maji, S.; López, I.; Meyer, S.; Meyer, F.; Llobet, A. *J. Am. Chem. Soc.* **2013,** *136*, 24-27.

(6) a) Sartorel, A.; Miró, P.; Salvadori, E.; Romain, S.; Carraro, M.; Scorrano, G.; Valentin, M. D.; Llobet, A.; Bo, C.; Bonchio, M. *J. Am. Chem. Soc.* **2009,** *131*, 16051-16053; b) Gersten, S. W.; Samuels, G. J.; Meyer, T. J. *J. Am. Chem. Soc.* **1982,** *104*, 4029-4030; c) Sens, C.; Romero, I.; Rodríguez, M.; Llobet, A.; Parella, T.; Benet-Buchholz, J. *J. Am. Chem. Soc.* **2004,** *126*, 7798-7799; d) Solomon, E. I.; Chen, P.;

Metz, M.; Lee, S.-K.; Palmer, A. E. *Angew. Chem. Int. Ed.* **2001,** *40*, 4570-4590; e) Thauer, R. K.; Klein, A. R.; Hartmann, G. C. *Chem. Rev.* **1996,** *96*, 3031-3042; f) Howard, J. B.; Rees, D. C. *Chem. Rev.* **1996,** *96*, 2965-2982; g) Wallar, B. J.; Lipscomb, J. D. *Chem. Rev.* **1996,** *96*, 2625-2658; h) Belle, C.; Pierre, J.-L. *Eur. J. Inorg. Chem.* **2003,** *2003*, 4137-4146.

(7) a) Nugent, J. H. A.; Ball, R. J.; Evans, M. C. W. *Biochim. Biophys. Acta, Bioenerg.* **2004,** *1655*, 217-221; b) Wilcox, D. E. *Chem. Rev.* **1996,** *96*, 2435-2458; c) Kitajima, N.; Moro-oka, Y. *Chem. Rev.* **1994,** *94*, 737-757; d) Magnus, K. A.; Ton-That, H.; Carpenter, J. E. *Chem. Rev.* **1994,** *94*, 727-735; e) Solomon, E. I.; Sundaram, U. M.; Machonkin, T. E. *Chem. Rev.* **1996,** *96*, 2563-2606; f) Mirica, L. M.; Ottenwaelder, X.; Stack, T. D. P. *Chem. Rev.* **2004,** *104*, 1013-1046; g) Lewis, E. A.; Tolman, W. B. *Chem. Rev.* **2004,** *104*, 1047-1076; h) Karlin, K. D.; Kopf, M.-A., *Biomimetic Oxidations Catalyzed by Transition Metal Complexes*; Imperial College Press: London, UK, 2000; i) Schindler, S. *Eur. J. Inorg. Chem.* **2000,** *2000*, 2311-2326; j) Nugent, J. H. A.; Rich, A. M.; Evans, M. C. W. *Biochim. Biophys. Acta, Bioenerg.* **2001,** *1503*, 138-146; k) Renger, G. *Biochim. Biophys. Acta, Bioenerg.* **2001,** *1503*, 210-228.

(8) Cramer, C. J.; Tolman, W. B. *Acc. Chem. Res.* **2007,** *40*, 601-608.

(9) a) Roeser, S.; Maji, S.; Benet-Buchholz, J.; Pons, J.; Llobet, A. *Eur. J. Inorg. Chem.* **2013,** *2013*, 232-240; b) Sens, C.; Rodríguez, M.; Romero, I.; Llobet, A.; Parella, T.; Sullivan, B. P.; Benet-Buchholz, J. *Inorg. Chem.* **2003,** *42*, 2040-2048.

(10) a) Planas, N.; Christian, G.; Roeser, S.; Mas-Marzá, E.; Kollipara, M.-R.; Benet-Buchholz, J.; Maseras, F.; Llobet, A. *Inorg. Chem.* **2012,** *51*, 1889-1901; b) Planas, N.; Christian, G. J.; Mas-Marzá, E.; Sala, X.; Fontrodona, X.; Maseras, F.; Llobet, A. *Chem. Eur. J.* **2010,** *16*, 7965-7968.

24

(11) a) Sens, C.; Rodríguez, M.; Romero, I.; Llobet, A.; Parella, T.; Benet-Buchholz, J. *Inorg. Chem.* **2003,** *42*, 8385-8394; b) Roeser, S.; Farràs, P.; Bozoglian, F.; Martínez-Belmonte, M.; Benet-Buchholz, J.; Llobet, A. *ChemSusChem* **2011,** *4*, 197-207.

(12) a) Schneider, B.; Demeshko, S.; Neudeck, S.; Dechert, S.; Meyer, F. *Inorg. Chem.* **2013,** *52*, 13230-13237; b) Kim, S. B.; Pike, R. D.; Sweigart, D. A. *Acc. Chem. Res.* **2013,** *46*, 2485-2497; c) Horike, S.; Umeyama, D.; Kitagawa, S. *Acc. Chem. Res.* **2013,** *46*, 2376-2384; d) Leong, W. L.; Vittal, J. J. *Chem. Rev.* **2010,** *111*, 688-764.

(13) Data collection with APEX II versions v2009.1-02 and v2013.4-1. Bruker (2007). Bruker AXS Inc., Madison, Wisconsin, USA.

(14) Data reduction with Bruker SAINT versions V7.60A and V8.30c. Bruker (2007). Bruker AXS Inc., Madison, Wisconsin, USA.

(15) SADABS: V2008/1 and V2012/1 Bruker (2001). Bruker AXS Inc., Madison, Wisconsin, USA; Blessing, Acta Crystallogr. A 1995, 51, 33.

(16) SADABS: V2008/1 and V2012/1 Bruker (2001). Bruker AXS Inc., Madison, Wisconsin, USA; Blessing, Acta Cryst. 1995, A51, 33.

(17) Sheldrick, G. *Acta Crystallogr. A* **2008,** *64*, 112-122.

(18) a) te Velde, G.; Bickelhaupt, F. M.; Baerends, E. J.; Fonseca Guerra, C.; van Gisbergen, S. J. A.; Snijders, J. G.; Ziegler, T. *J. Comput. Chem.* **2001,** *22*, 931-967; b) Fonseca Guerra, C.; Snijders, J. G.; te Velde, G.; Baerends, E. J. *Theor. Chem. Acc.* **1998,** *99*, 391-403.

(19) Becke, A. D. *Phys. Rev. A* **1988,** *38*, 3098-3100.

(20) a) Perdew, J. P. *Phys. Rev. B* **1986,** *33*, 8822-8824; b) Perdew, J. P. *Phys. Rev. B* **1986,** *34*, 7406-7406.

(21) a) Lenthe, E. v.; Baerends, E. J.; Snijders, J. G. *J. Chem. Phys.* **1993,** *99*, 4597-4610; b) van Lenthe, E.; Baerends, E. J.; Snijders, J. G. *J. Chem. Phys.* **1994,** *101*, 9783-9792.

(22) Grimme, S. *J. Comput. Chem.* **2006,** *27*, 1787-1799.

(23) Teixidor, F.; Garcia, R.; Pons, J.; Casabó, J. *Polyhedron* **1988,** *7*, 43-47.

(24) a) Maji, S.; López, I.; Bozoglian, F.; Benet-Buchholz, J.; Llobet, A. *Inorg. Chem.* **2013,** *52*, 3591-3593; b) Farràs, P.; Maji, S.; Benet-Buchholz, J.; Llobet, A. *Chem. Eur. J.* **2013,** *19*, 7162-7172; c) Romero, I.; Rodriguez, M.; Llobet, A.; Collomb-Dunand-Sauthier, M.-N.; Deronzier, A.; Parella, T.; Stoeckli-Evans, H. *J. Chem. Soc., Dalton Trans.* **2000**, 1689-1694.

(25) a) Solans, X.; Font-Altaba, M.; Briansó, J. L.; Llobet, A.; Teixidor, F.; Casabó, J. *Acta Crystallogr. C* **1983,** *39*, 1512-1514; b) Gao, C.-Y.; Qiao, X.; Ma, Z.-Y.; Wang, Z.-G.; Lu, J.; Tian, J.-L.; Xu, J.-Y.; Yan, S.-P. *Dalton Trans.* **2012,** *41*, 12220-12232; c) Trivedi, M.; Pandey, D. S.; Rath, N. P. *Inorg. Chim. Acta* **2009,** *362*, 284-290.

(26) a) Haga, M.; Dodsworth, E. S.; Lever, A. B. P. *Inorg. Chem.* **1986,** *25*, 447-453; b) Wong, C.-Y.; Che, C.-M.; Chan, M. C. W.; Leung, K.-H.; Phillips, D. L.; Zhu, N. *J. Am. Chem. Soc.* **2004,** *126*, 2501-2514; c) Kannan, S.; Ramesh, R.; Liu, Y. *J. Organomet. Chem.* **2007,** *692*, 3380-3391.

(27) a) Gilbert, J. A.; Eggleston, D. S.; Murphy, W. R.; Geselowitz, D. A.; Gersten, S. W.; Hodgson, D. J.; Meyer, T. J. *J. Am. Chem. Soc.* **1985,** *107*, 3855-3864; b) Llobet, A.; Curry, M. E.; Evans, H. T.; Meyer, T. J. *Inorg. Chem.* **1989,** *28*, 3131-3137; c) López, I.; Ertem, M. Z.; Maji, S.; Benet-Buchholz, J.; Keidel, A.; Kuhlmann, U.; Hildebrandt, P.; Cramer, C. J.; Batista, V. S.; Llobet, A. *Angew. Chem. Int. Ed.* **2014,** *53*, 205-209.

(28) a) Ahmed, H. M. Y.; Coburn, N.; Dini, D.; de Jong, J. J. D.; Villani, C.; Browne, W. R.; Vos, J. G. *Inorg. Chem.* **2011,** *50*, 5861-5863; b) Halpin, Y.; Dini, D.; Younis Ahmed, H. M.; Cassidy, L.; Browne, W. R.; Vos, J. G. *Inorg. Chem.* **2010,** *49*, 2799-2807.

(29) a) Baitalik, S.; Florke, U.; Nag, K. *J. Chem. Soc., Dalton Trans.* **1999**, 719-728; b) Brietzke, T.; Mickler, W.; Kelling, A.; Schilde, U.; Krüger, H.-J.; Holdt, H.-J. *Eur. J. Inorg. Chem.* **2012,** *2012*, 4632-4643; c) Browne, W. R.; Hage, R.; Vos, J. G. *Coord. Chem. Rev.* **2006,** *250*, 1653-1668; d) D'Alessandro, D. M.; Keene, F. R. *Chem. Soc. Rev.* **2006,** *35*, 424-440; e) D'Alessandro, D. M.; Keene, F. R. *Chem. Eur. J.* **2005,** *11*, 3679-3688; f) Das, A.; Kundu, T.; Mobin, S. M.; Priego, J. L.; Jimenez-Aparicio, R.; Lahiri, G. K. *Dalton Trans.* **2013,** *42*, 13733-13746; g) Kundu, T.; Schweinfurth, D.; Sarkar, B.; Mondal, T. K.; Fiedler, J.; Mobin, S. M.; Puranik, V. G.; Kaim, W.; Lahiri, G. K. *Dalton Trans.* **2012,** *41*, 13429-13440; h) Mandal, A.; Agarwala, H.; Ray, R.; Plebst, S.; Mobin, S. M.; Priego, J. L.; Jiménez-Aparicio, R.; Kaim, W.; Lahiri, G. K. *Inorg. Chem.* **2014,** *53*, 6082-6093; i) Mondal, P.; Agarwala, H.; Jana, R. D.; Plebst, S.; Grupp, A.; Ehret, F.; Mobin, S. M.; Kaim, W.; Lahiri, G. K. *Inorg. Chem.* **2014,** *53*, 7389-7403; j) Roeser, S.; Ertem, M. Z.; Cady, C.; Lomoth, R.; Benet-Buchholz, J.; Hammarström, L.; Sarkar, B.; Kaim, W.; Cramer, C. J.; Llobet, A. *Inorg. Chem.* **2011,** *51*, 320-327.

(30) Romain, S.; Rich, J.; Sens, C.; Stoll, T.; Benet-Buchholz, J.; Llobet, A.; Rodriguez, M.; Romero, I.; Clérac, R.; Mathonière, C.; Duboc, C.; Deronzier, A.; Collomb, M.-N. l. *Inorg. Chem.* **2011,** *50*, 8427-8436.
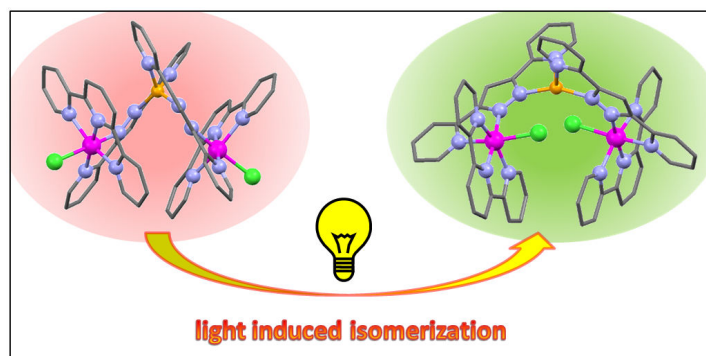
27

For Table of Contents Only

light induced isomerization

Table of Content Synopsis:

The coordination chemistry of new dinuclear Ru-Zn and self-assembled hetero-trinuclear Ru$_2$-Zn complexes that contain the Hbpp ligand have been thoroughly characterized by means of spectroscopic and electrochemical techniques. Additionally, a light induced linkage isomerization reaction has been shown to occur for the Ru-Cl heterotrinculear complexes.